(019)

A Low Cost Ultrasound-based Localisation System

A. Burns, S. Fichera and P. Paoletti
School of Engineering, University of Liverpool, Brownlow Hill, Liverpool L69 3GH, UK
Tel.: +44 151 7945232
E-mail: P.Paoletti@liverpool.ac.uk

Summary: This paper presents a low-cost localisation system based on ultrasonic sensing and time of flight measurements. A compact ultrasound emitter has been designed to generate omnidirectional trains of ultrasound pulses which are then picked up by several fixed receivers measuring time difference of arrival. A least squares approach is used to analytically obtain a first estimate of the emitter position, which is then refined through steepest descent optimisation. All processing is done via a standard Arduino platform, proving the low computational demands of the method. Localisation results are validated against a state-of-the-art Optitrack motion capture system. It is shown that the system can cover a 4.3×3.1 m arena with a mean error localisation error of 1.57 cm and an average standard deviation of 1.39 cm throughout the arena.

Keywords: Localisation, Ultrasound, Time difference of arrival, Positioning.

1. Introduction

Being able to localise markers and devices is a critical enabling technology for a wide variety of fields, spanning biomechanics, robotics, sensor networks, etc. Over the years, several methods have been developed to tackle the localization challenge. Localisation platforms based on external sensory networks may provide an effective solution for satisfying accuracy requirements while meeting low-cost constraints.

In this work, a novel low-cost localisation system based on ultrasound sensing is described and validated against a state-of-the-art motion tracking system. It is shown that such localisation platform is able to provide good accuracy while requiring very limited sensing and computational complexity.

2. Definition of the Infrastructure

Various factors need to be taken into consideration when designing or assessing any localisation technique, including: accuracy, precision, robustness, financial cost and system simplicity (refer to [1] for definitions of these metrics). Wireless indoor localisation approaches can be classified according to two main criteria [1, 2]: i) Physical sensor infrastructure, i.e. the platform used to detect/sense position, and ii) Positioning algorithm, i.e. the method to estimate location from sensory data.

Most physical sensory infrastructures rely on: a signal generator, called an emitter, and a measuring unit, called a receiver. Measurement involves the transmission and reception of signals between these parts of the system. There are four different system topologies for positioning systems [2]. An Indirect Remote Positioning System (IRPS) was selected here as it reduces the need for the mobile system to have high computational capabilities on board and offsets this function to a fixed ground station. This widens the range of systems the localisation platform could be applied to.

Within the IRPS family of localisation systems, different choices of signals propagated between the emitter and receivers can be made. Here, ultrasound (US) localisation was selected as the most appropriate sensor type due to its potential high accuracy and low cost. Furthermore, due to the slow propagation speed of US waves (340 m/s), simple processing technology can be used, reducing overall complexity. The drawback of currently available systems are overall cost and scalability [3, 4]. In fact, the use of the ultrasonic sensing within an IRPS topology is a largely unexplored technique, due to the challenge of having a pointwise omnidirectional US emitter alongside a communication system to transmit localisation data back to the mobile system. The system proposed here overcomes these issues, maintaining high accuracy on large volumes while being significantly less expensive than commercially available platforms. In particular, this is achieved by i) designing a central 'omnidirectional' ultrasonic emitter, described in Section 4, ii) using computationally cheap position estimation algorithms that can run on simple microcontrollers (Section 3), which are then interfaced with iii) an embedded radio communication system (Section 4).

3. Localization Estimation Algorithm

The proposed system consists of a central 'omnidirectional' point emitter to be localised and a series of fixed directional receivers at known locations.

Time-Difference-of-Arrival (TDoA) was selected as the approach to estimate emitter position. When compared with other approaches such as Angle-of-Arrival or Time-of-Arrival, TDoA systems are cheaper and simpler in both hardware and computational algorithm [4-6]. For TDoA, an omnidirectional US

signal is generated from the mobile emitter. As this pulse reaches the first receiver, the time of reception t_0 is recorded. Furthermore, as the US pulse continues to travel, it will continue triggering receivers which will also record times *relative* to the first receiver $t_{i0} = t_i - t_0$. These relative times of reception allow localization of the emitter on a hyperboloid with the first receiver and the i-th receiver positions as foci [7]. Mathematically, this translates into the system of equations [8]

$$\begin{aligned} (x-x_0)^2+(y-y_0)^2+(z-z_0)^2 &= (t_0+t_{00})^2 v_s^2 \\ (x-x_1)^2+(y-y_1)^2+(z-z_1)^2 &= (t_0+t_{10})^2 v_s^2 \\ &\vdots \\ (x-x_i)^2+(y-y_i)^2+(z-z_i)^2 &= (t_0+t_{i0})^2 v_s^2 \end{aligned}, \quad (1)$$

where v_s is the speed of the US signal, (x,y,z) are the unknown emitter coordinates and (x_i, y_i, z_i) are the known positions of the receivers. Note that $t_{00} = 0$ by definition.

3.1. Initial Localisation via Triangulation

The physical infrastructure described in Section 2 and the TDoA approach described in Section 3 provides a series of hyperboloids theoretically intersecting only at the emitter location. However, noise in signal propagation, received signal measurement and receivers' locations translates to an uncertainty in the estimation of emitter position. Closed-form solutions for the localisation problem do not accommodate for situations where hyperboloids do not intersect at a single point [9], therefore best approximations algorithms are always necessary. An analytical solution to best-fit the emitter position in TDoA systems has been proposed in [8] and is used as a first step in the algorithm proposed in this paper.

To this end, the first line of equation (1) is subtracted from the subsequent lines, thus obtaining

$$2A\boldsymbol{p} = \boldsymbol{b}, \quad (2)$$

where

$$A = \begin{bmatrix} x_1' & y_1' & z_1' & t_{10}v_s^2 \\ x_2' & y_2' & z_2' & t_{20}v_s^2 \\ & \vdots & & \\ x_i' & y_i' & z_i' & t_{i1}v_s^2 \end{bmatrix}, \boldsymbol{p} = \begin{bmatrix} x \\ y \\ z \\ t_0 \end{bmatrix},$$
$$\boldsymbol{b} = \begin{bmatrix} x_1^2 - x_0^2 + y_1^2 - y_0^2 + z_1^2 - z_0^2 - t_{10}v_s^2 \\ x_2^2 - x_0^2 + y_2^2 - y_0^2 + z_2^2 - z_0^2 - t_{20}v_s^2 \\ \vdots \\ x_i^2 - x_0^2 + y_i^2 - y_0^2 + z_i^2 - z_0^2 - t_{i0}v_s^2 \end{bmatrix}, \quad (3)$$

and $x_i' = x_i - x_0, y_i' = y_i - y_0, z_i' = z_i - z_0$.

The solution of this system of linear equations then provides the emitter position $\boldsymbol{p}$. As mentioned before, presence of noise and uncertainties implies that no exact solution exists, therefore a Least Squares algorithm was used here to solve (2) with minimal computational cost [10]

$$\boldsymbol{p} = \left(\frac{1}{2}\right)(A^T A)^{-1} A^T(\boldsymbol{b}), \quad (4)$$

Note that this solution is simpler than the one described in the literature as it provides $\boldsymbol{p}$ in a single step and does not involve second order equations which may lead to multiple solutions. However, as matrix inversion $(A^T A)$ is required, the matrix $A^T A$ must be non-singular. According to the definition of the matrix A in (3), singular configurations may occur if, for example, all the receivers lay on the same plane (in this case one of the first three columns is zero), or if more than *N-4* receivers are located at the same point (in this case *N-4* rows are linearly dependent). These pathological situations can be easily avoided by placing the receivers accordingly. Lastly, errors will occur if all values of the fourth column of matrix A are *exactly* the same, that is if all receivers are the exact same distance away from the closest receiver to the robot. Once again, this situation is unlikely to occur in practice if the receivers are positioned correctly. Therefore equation (4) provides a robust and fast method to obtain a first estimate of the emitter location.

The solution proposed here, unlike the one described in [8], is based on a system that relies on one emitter and multiple receivers, with the algorithm being shaped on this assumption. The use of a single central emission pulse per cycle avoids the need for time scheduling between different transmitters. On the other hand, the system described in [8] requires a 65 ms time allocation per emitter, reducing overall scalability. Moreover, the solution proposed here removes the requirement for the ultrasonic transmitters to emit signals with known periods and order, thus further reducing system complexity.

3.2. Localisation Improvement via Optimization

There are several sources of noise and uncertainty in the system, therefore an optimisation procedure is used to minimise the effect on such factors on localisation accuracy. The algorithm described in Section 3.1 provides a good first estimate of the emitter location, but the presence of noise and uncertainty limits its accuracy. Therefore, the estimate obtained in (4) is used as first guess in an iterative optimization procedure aimed at improving localisation accuracy by adjusting the estimate $\boldsymbol{p}$. Such an optimization problem can be mathematically expressed as

$$\boldsymbol{p_{estimated}} = argmin_{\tilde{\boldsymbol{p}}_0}[S(\boldsymbol{p})], \quad (5)$$

$$S(\boldsymbol{p}) = \sum_{i=1}^{N} [(x-x_i)^2 + (y-y_i)^2 + (z-z_i)^2 - (t_0 + t_{i0})^2 v_{sound}^2]^2 \quad (6)$$

A simple steepest descent algorithm is proposed to solve such problem. Note that Gauss-Newton or Levenberg-Marquardt are often preferred thanks to their superior convergence properties [11], but they require significantly more computational and memory resources. Moreover, simulation results indicate that such more advanced methods do not offer improved performance compared to the simpler steepest descent method for the localisation scenario considered here.

The pseudo-code of the implemented steepest descent algorithm proposed for the localisation platform is shown in Table 1. Both the step size and the stopping criterion for these experiments were chosen heuristically. The step size was optimized to ensure convergence without requiring too many steps and the stopping criterion ensures that the iterative minimiser stops as soon as convergence occurs. The constraint $k < k_{max}$ is included to terminate the iterative process so that there exists an upper bound for its execution time. In fact, very often (e.g. for real mobile robotic control) it is more important to get position estimates with a good rate, even at the expenses of accuracy. Moreover, it is worth noting that most of the benefits of steepest descent are realised in the first few iterations [11], therefore even a small value of k_{max} is sufficient to significantly improve accuracy with respect to the estimate provided by (4).

Table 1. Pseudo-code for solving problem (5)-(6).

1. Initialise $\boldsymbol{p_{estimated}}(1)$ with results from equation (4);
2. Calculate step direction $\boldsymbol{step}(k) = -\nabla S(\boldsymbol{p_{estimated}}(k))$;
3. Perform an optimisation step, with a predetermined step size α
$$\boldsymbol{p_{estimated}}(k+1) = \alpha \cdot \boldsymbol{step}(k) + \boldsymbol{p_{estimated}}(k);$$
4. Check the stopping criterion for convergence;
5. If the stopping criterion is not satisfied and $k < k_{max}$ repeat steps 2-5, otherwise return $\boldsymbol{p_{estimated}}(k)$.

For the results shown in this paper we used $k_{max} = 40$ and the stopping criterion $|\boldsymbol{p_{estimated}}(k) - \boldsymbol{p_{estimated}}(k-1)| < 0.0002$. On the standard Arduino Mega 2560 platforms used for validation it takes on average 0.7 s to get the final estimate for emitter location, of which about 0.3 s are spent for running the minimisation algorithm.

4. Experimental Setup for Validation

4.1. Setup

The processor unit utilised is an Arduino Mega 2560, which detects signals from the receivers and runs algorithm 1 and 2 for localisation. The output of this Arduino is connected to a Raspberry Pi to transmit all coordinates to a laptop to make a comparison with the coordinates provided by a motion tracking system composed of 8 Optitrack Prime 17 W cameras. The emitter unit also utilizes an Arduino Mega 2560 board to trigger emission. Both units are connected via an RF transmitter/receiver (ERA-ARDUINO-S900) to trigger a new emission only once the localisation algorithm is finished. Motion capture results are captured at 100 Hz, whereas algorithm 2 takes about 0.7 s to run on the Arduino Mega 2560 board. To synchronise these two datasets, motion capture results are acquired and stored until the localiser has calculated a position, and then the nearest pair of coordinates from the 10 most recently acquired points is chosen to perform the comparison. Note that the robot used for moving the emitter has a speed of less than 1 cm/s, therefore such synchronisation strategy is accurate.

4.2. Hardware

The 12 receivers used are based on US ceramic transducers (MCUSD16A40S12RO), which resonate at 40 kHz when detecting the pulse generated by the emitter. The received signal is then amplified 8-fold by a three stage analogue amplifier and then converted to a square wave via a Schmidt-comparator (LM386). This signal processing electronics was inspired by the one described in [12]. The threshold value of the Schmidt-comparator was chosen to maximise range while avoiding the possibility of signal noise being amplified. For the setup described in this paper, values between ~0.04 V and ~0.9 V provided a good trade-off between range and noise removal. This output of the Schmidt-comparator is then rectified and filtered by a passive Low Pass Filter at 15.9 kHz. Finally, a comparator (LM339-N) with cut off voltage is 1.9 V is used to generate the trigger signal to be transmitted to the processing unit.

The emitter is a composed by 13 US transducers (MCUSD16A40S12RO), with their outer metallic case removed to reduce the directionality properties. The support for such transducer was designed and 3D-printed so that an (almost) omnidirectional emission was achieved, as shown in Fig. 1. By doing this, the emitter can be considered a point source as required by the localisation algorithm described in Section 3. The 13 transducers are simultaneously pulsed using a microcontroller (PIC12F1822) generating a 40 kHz square wave, which is then amplified via a MOSFET amplifier and fed to the US emitters.

Experimental tests highlighted that the number of pulses driving the emitters affects the performance of the localisation system both in in terms of coverage and accuracy. More pulses result in increased coverage but decreased accuracy, and vice versa. As reported in Fig. 2, the mean overall error across the arena is proportional to the number of pulses. When a single pulse is emitted, the initial time t_0 will be identical for any active receiver. However, if there are two pulses

and some receivers pick up the first pulse and some receivers pick up the second pulse, then t_{i0} may be different for these two sets of receivers, thus introducing additional uncertainty and increasing the localisation error. This effect may become significant for larger numbers of pulses. In fact, at 40 kHz, the time between pulses is 12.5 μs, which corresponds to 4.3 mm/pulse with a speed of sound $v_{sound} = 343\, m/s$. However, this uncertainty is significantly mitigated by the optimiser. On the other hand, the coverage of the system relies solely on the number of receivers picking up a signal at any given emission. Given the receiver circuits used, a weak reception may not always be immediately detected from the first pulse and could take multiple pulses from the same signal before detection is triggered. Therefore, the more pulses are being transmitted, the more likely a receiver will register a reception and the higher the coverage is, as shown in Fig. 2. The optimal number of pulses for the setup used for validation was determined to be five to ensure almost complete coverage while retaining good accuracy.

Fig. 1. 'Omnidirectional' US transducer array for the emitter.

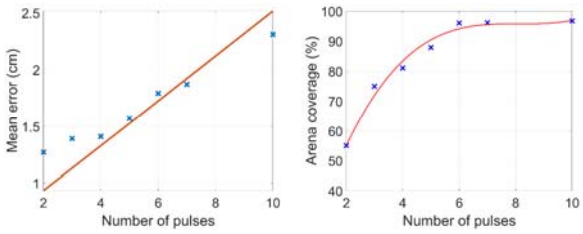

Fig. 2. Mean error (cm, left) and arena coverage (%, right) vs. number of pulses.

5. Results

Testing was done in a motion capture arena of approximately 4.3 m by 3.1 m, the emitter unit was placed onboard a Create 2 Programmable Robot (iRobot, USA) that performed random movement around the arena for up 1 hour per test. The results from both the localiser and motion capture were stored offline during this time. The system was tested at four different emitter heights from the floor: 280 mm, 355 mm, 457 mm and 592 mm, to prove its robustness. A summary of the results obtained of these experiments is reported in Table 2.

The 'pre-minimiser results' are obtained using equation (4), whereas results from the optimization routine described in Section 3 are referred as 'post-minimiser results'. Finally, given that the robot cannot move faster than approximately 1 cm/s and that algorithm 2 provide results every 0.7 seconds, any localisation estimate that is more than 15 cm apart from the last estimate can be considered as outlier and removed. Such outlier removal provides the set of 'post-filter results'. As can be seen in Table 1, localisation performance has similar trends across all the tested heights. In the following, only the results attained at 355 mm altitude are reported as illustrative examples.

Table 2. Localisation results at different heights.

Height (mm)	Mean Error *Post-Filt (cm)*	Points with error < 1 cm *Post-Filt* (%)	Points with error < 3 cm *Post-Filt* (%)	Cover age (%)
280	1.61	40.1	87.9	87.87
355	1.57	43.05	88.69	93.40
457	1.81	36.43	85.45	86.27
592	1.62	41.06	89.08	79.40

5.1. Pre-minimiser

The pre-minimiser results obtained by (4) and shown in Fig. 3 are quite inaccurate. In fact, only 14.2 % of the results are within 1 cm of the true position, 47.8 % are within 3 cm and 81.5 % are within 10 cm. The mean error across all attained values is 11.2 cm. Such relatively high mean localisation error is significantly affected by the presence of extremely large errors (>30 cm) due to emitter reflections being picked up on the receiver units, a phenomenon that will be further discussed later.

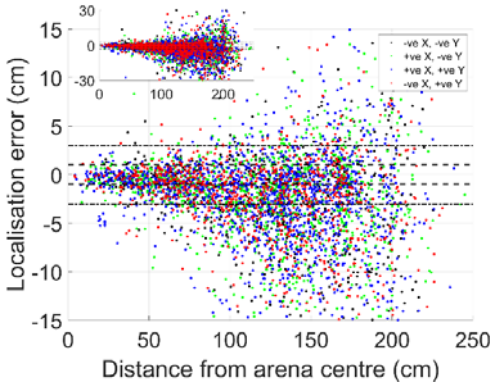

Fig. 3. Pre-Minimiser localisation error (cm) vs Distance from Arena Centre, where different colours are used for the four quadrants of the arena. Inset plot shows a zoomed-out view of the localisation error (range ±30 cm).

Another noticeable trend is the monotonic increase of error spread as a function of distance from the centre of the arena. This is likely due to the number of receivers being involved in a positional calculation; as the robot moves away from the centre, some receivers go out of range and therefore less information is provided to the localisation algorithm.

Note that there exist spurious error clusters in certain quadrants, as highlighted in Fig. 4. Upon further inspection, these outliers were the results of some receivers picking up a reflected emission rather than the actual emission. In certain areas, this will happen in such a way that both algorithms will converge on an incorrect location. This could be mitigated by increasing delays between emission, by logic filtering or by reducing emission strength to decrease reflection likelihood.

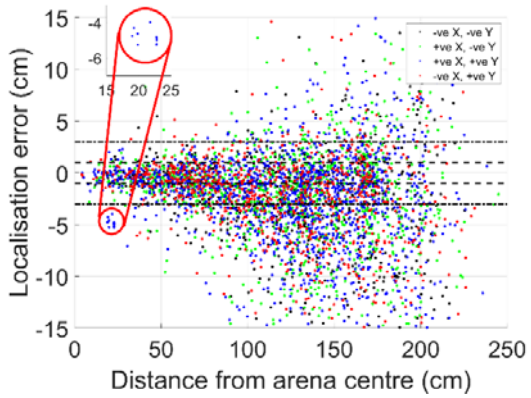

Fig. 4. Highlighted area of reflected reception.

To better quantify accuracy, the heat map shown in Fig. 5 was produced by discretizing the arena on a grid whose cells are 40 cm wide and reporting the median localisation error value for each cell. An 'Inf' value within a cell represents an area that has not been explored by the mobile robot during tests, and it is not taken into account when calculating means. The colour scaling is based on how accurate the data is.

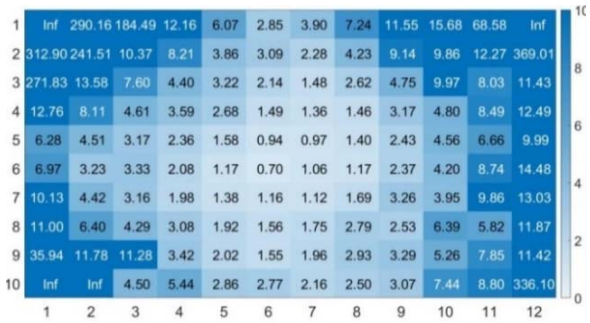

Fig. 5. Pre-Minimiser heatmap of the median localisation error across the arena. Each cell represents a 40 cm × 40 cm region in the arena.

5.2. Post Minimiser

After processing the results through the algorithm reported in Table 1, 41.7 % of the results are within 1 cm of the true position, almost 3 times as many as the pre-minimised results. Moreover, 85.9 % of results are now within 3 cm and 96.4 % are within 10 cm of true position. Such an improved performance translates to an average mean error of 3.33 cm. As shown in Fig. 6, the post minimiser results are more accurate throughout the arena, and the error does not significantly increase as the emitter moves away from the centre of the arena.

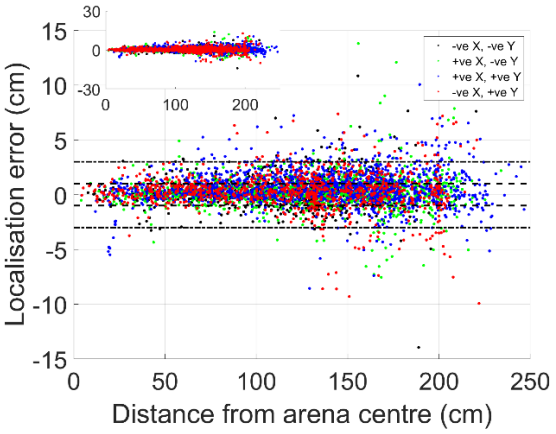

Fig. 6. Post-Minimiser localisation error (cm) vs Distance from Arena Centre where different colours are used for the four quadrants of the arena. Inset plot shows a zoomed-out view of the localisation error (range ±30 cm).

The heat map shown in Fig. 7 demonstrates that the vast majority of results lie well within acceptable tolerances, with only 5 out of 120 cells having median errors above 5 cm.

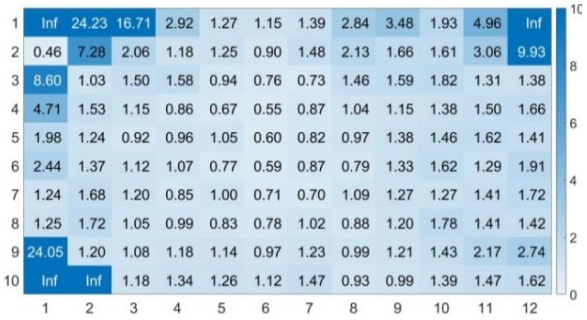

Fig. 7. Post-Minimiser heatmap of localisation error across the arena, showing median results for quadrants of 40 cm × 40 cm.

5.3. Post Filter

When applying the final filter to remove any value that differs more than 15 cm from the previous estimate, the accuracy improves even further: 43.1 % of the results are within 1 cm of the true position, 88.7 % are within 3 cm and 99.5 % are within 10 cm. The overall average mean error drops to 1.57 cm as well. Fig. 8 reports the heat map related to these results.

Fig. 9 reports the median error (blue dots and lines) and the mean error (red dots and line) as functions of distance from the arena centre. Both trends can be fitted by quadratic polynomials with the mean error showing some anomalies at 20 cm from arena centre, which result from the clustered reflections described earlier. The median result is far more robust to such reflection areas and shows a consistently lower error

throughout the arena, indicating that the error distribution is skewed. The standard deviation of the results also increased with distance from arena centre, with an average standard deviation throughout the arena of 1.39 cm.

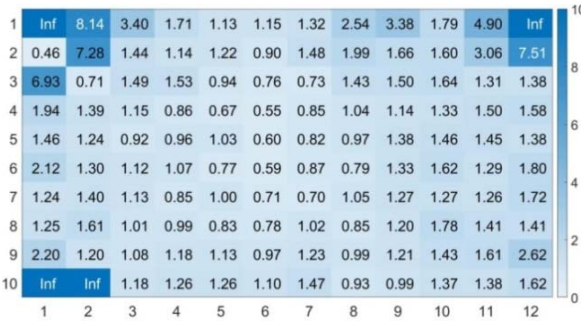

Fig. 8. Post-Filter heatmap of localisation error across the arena, showing median results for quadrants of 40 cm × 40 cm.

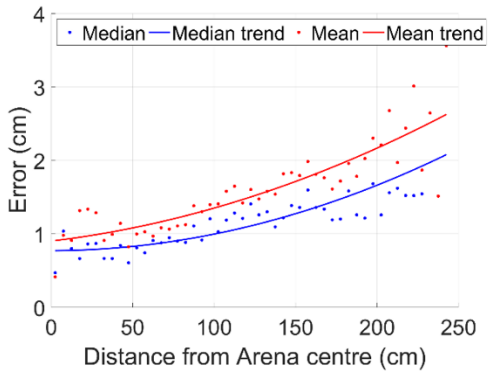

Fig. 9. Median error (red) and mean error (blue) vs distance from arena centre.

5.4. Results Summary

Table 3 summarises the results of each stage of processing, highlighting that the minimisation and filtering algorithms significantly improve localisation performance.

Table 3. Summary of results obtained at various processing stages. E = Error, Min = Minimiser, Filt = Filter.

	Mean E	E < 1 cm	E < 3 cm	E < 10 cm
Pre-Min	11.2 cm	14.2 %	47.8 %	81.5 %
Pre-Filt	3.33 cm	41.7 %	85.9 %	96.4 %
Post	1.57 cm	43.1 %	88.7 %	99.5 %

As previously mentioned, reflections played a major role in certain areas and significantly affected accuracy in these areas. One way in which this could be mitigated would be the addition of a constant time delay to ensure the dissipation of any remnant signals from previous pulses. Usage in open outdoor areas would also remove any reflective areas.

6. Conclusions

In this paper an inexpensive yet accurate ultrasound-based localisation system is proposed. The total cost of the components is around £100, the biggest share of which are two Arduino Mega 2560 boards used for trigger emission and for processing data at the receivers end. The system allows localisation of 89 % of the 4.3 m × 3.1 m with an accuracy of less than 3 cm and 43 % with an accuracy of less than 1 cm. The system has been proven to be scalable between 280 mm and 592 mm of height, without requiring any change in the experimental setup. Given the range of the ultrasound transceivers used, the system should theoretically perform well in arenas up to 12×12×12 m in size. Optimisation of receiver location and orientation, and use of more powerful transducer, can also allow better performance in larger arenas if needed. Finally, more advanced filtering approaches may be developed to improve robustness with respect to spurious reflections. Application in alternative domains, such as camera-less surveillance systems to improve privacy, may be considered as well.

Acknowledgements

This research was supported by Apadana Management 3 Ltd. The authors also wish to thank colleagues from the University of Liverpool who provided insight and expertise that greatly assisted the research.

References

[1]. H. Liu, H. Darabi, P. Banerjee and J. Liu, Survey of wireless indoor positioning techniques and systems, *IEEE Trans. Syst., Man, Cybern.,* Vol. 37, Issue 6, 2007, pp. 1067-1080.

[2]. E. Tinti, Metodi e Stumenti per il Posizionamento Indoor, *Università di Bologna-Campus Di Cesena – Scuola Di Scienze*, Bologna, 2014.

[3]. R. Brena, et al., Evolution of indoor positioning technologies: A survey, *J. Sensors*, Vol. 2017, 2017, 2630413.

[4]. A. A. Khudhair, S. Q. Jabbar, M. Q. Sulttan, D. Wang, Wireless indoor localization systems and techniques: Survey and comparative study, *Indonesian J. of Elect. Eng. and Computer Sci.,* Vol. 3, Issue 2, 2016, pp. 392-409.

[5]. A. Yassin, et al., Recent Advances in indoor localization: A survey on theoretical approaches and applications, *IEEE Commun. Surveys Tuts.,* Issue 19, 2017, pp. 1327-1246.

[6]. G. Mao, B. Fidan, Localization Algorithms and Strategies for Wireless Sensor Networks, *Information Science Reference-Imprint of IGI Publishing,* 2009.

[7]. R. Kaune, J. Horst, W. Koch, Accuracy analysis for TDOA localization in sensor networks, in *Proceedings of the 14th Int. Conference on Information Fusion*, Chicago, Illinois, USA, 2011, pp. 1-8.

[8]. U. Yayan, H. Yucel, A. Yazici, A low cost ultrasonic based positioning system for the indoor navigation of mobile robots, *J. Intell. Robotic Syst.*, Vol. 78, Issue 3, 2015, pp. 541-552.

[9]. Y. Zhou, An efficient least-squares trilateration algorithm for mobile robot localization, in *Proceedings of the IEEE/RSJ Int. Conference on Intell. Robots and Systems (IROS'09)*, 2009, pp. 3474-3479.

[10]. K. W. Cheung, H. C. So, W.-K. Ma, Y. T. Chan, A constrained least squares approach to mobile positioning, *EURASIP J. on Appl. Signal Proc.*, 2006, pp. 1-23.

[11]. S. J. Wright, J. Nocedal, Numerical Optimization, *Springer*, 1999.

[12]. Engineeringshock Electronics, http://www.engineeringshock.com/ultrasonics.html